The Spacecraft Antennas

By J. T. BANGERT, R. S. ENGELBRECHT, E. T. HARKLESS, R. V. SPERRY and E. J. WALSH

(Manuscript received February 13, 1963)

The spacecraft employs two microwave antennas for communications and a single VHF antenna for telemetry, beacon, and command functions. One microwave antenna centered at 6 gc is used to receive broadband signals from a ground transmitter while the other microwave antenna centered at 4 gc is used to transmit signals to a ground receiver. Each microwave antenna is composed of a large number of circularly polarized radiating elements equally spaced around the equator of the spacecraft and connected to the electronic receiver and transmitter by a complex precision feed system. The VHF antenna is a small multi-element helix mounted at the pole of the spacecraft and radiates a linearly polarized signal. All antennas provide nearly isotropic antenna patterns with the axis of symmetry corresponding to the spin axis of the spacecraft. The antenna systems were constructed of light, but rugged, materials and passed extensive electrical, mechanical, and thermal tests.

I. INTRODUCTION

The function of the spacecraft antennas is to receive and transmit two distinct classes of signals: broadband microwave frequencies for communication service, such as television; and narrow-band VHF for beacon, command, and telemetry.

The requirements on these antennas resulted from a thorough systems analysis which led to an intricate balance of many factors involving not only the spacecraft, but the ground station as well.

These factors include such vital questions as: the modulation method, the location of frequencies, the choice of polarizations, the degree of attitude stabilization, etc., and are discussed in companion papers.[1,2,3]

1.1 *Requirements*

One of the most important and difficult objectives was to make the patterns provided by both the microwave and VHF antennas as nearly

isotropic as possible. This is necessary because the spacecraft is spin stabilized; consequently the received and transmitted signal amplitudes will fluctuate by an amount depending on the anisotropy of the antenna pattern. In addition, the microwave antenna must receive right circularly polarized FM signals centered at 6390 mc and transmit left circularly polarized FM signals centered at 4170 plus a beacon signal at 4080 mc. The wide frequency separation and the opposite sense of circular polarization for the 4- and 6-gc signals suggests two microwave antennas. A single VHF antenna is used to receive command signals at 123 mc and to transmit a 136-mc beacon which can be amplitude modulated with telemetry information.

In a realistic allocation of the extremely valuable space in the spacecraft, the microwave antennas were assigned a band around the equator. This band had an outside diameter of 34.5 inches, a height of 6 inches, and a depth of 3 inches. In addition, a few extra cubic inches were available in the interior for the needed feed system. It was decided to mount the VHF antenna projecting outward from the top of the spin axis. All three antennas are shown in Fig. 1. The satellite maximum mass was

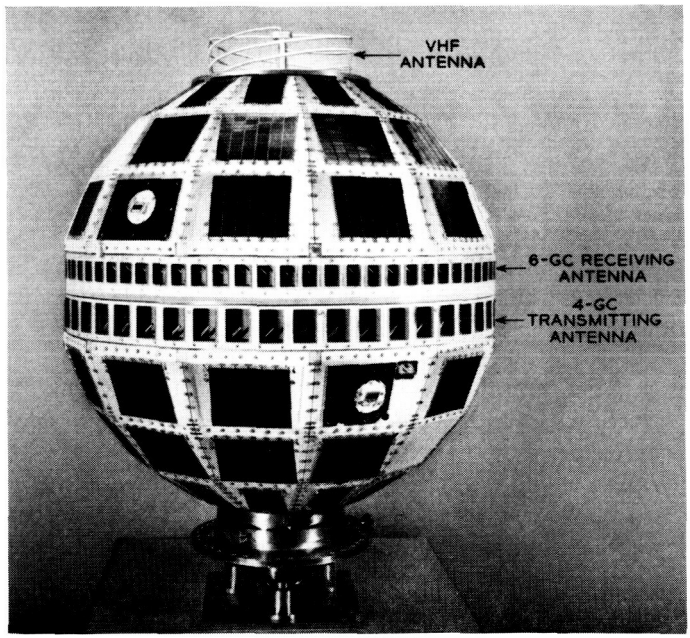

Fig. 1 — Spacecraft, showing microwave antennas and VHF antenna.

determined by the launch vehicle capabilities. The guiding design rule was that every item in the satellite was to be as light as possible. About 7 pounds was allotted to the complete antenna system. The completed satellite also had to be balanced and have a moment of inertia with respect to its spin axis such that there would be no tumbling effect while in orbit.

In addition to fulfilling the system's electrical performance requirements, the construction of the antennas had to be such that they would withstand the induced vibrational stresses of the launching and then continue at the desired level of performance in the high vacuum and extreme temperature variations of outer space. Furthermore, the antennas had to be able to withstand the high-energy nuclear particles as well as the low-energy microscopic particles found in space.

One of the most serious constraints affecting the antenna design was the necessity of building a full-scale electrical model in a total of twenty working days. It is clear that under such time pressure there was no opportunity to explore elegant proposals or to debate several alternatives. Only the most straightforward approach offering the highest probability of success could be pursued. An essential factor in the development was reliability. When reliability and urgency are both needed, new and unproven methods and materials are used only as a last resort. All materials and techniques, where possible, were proven ones. Those which were new were life tested within the limits allowed by the program's rapid pace.

A minor complication was the added requirement that the top and bottom hemispheres of Telstar be dc isolated from each other in order to reduce the eddy current damping of the spin energy. A continuous strip of insulated conductor was provided on the edge of the 4-gc radiator band to provide a bypass capacitor. Spring fingers on the 6-gc band provided continuous contact to one terminal of this RF bypass capacitor. A further complication was the need for the VHF antenna to operate during the launching operations.

Since the microwave antennas and the VHF antenna are distinct and independent systems, each will be described in separate sections of this paper.

II. MICROWAVE ANTENNA SYSTEM

The two microwave antenna systems shown schematically in Fig. 2 are each composed of an array of discrete radiating elements and a complex power distribution system to supply each element. The power distribution system consists of both resistive and reactive power dividers

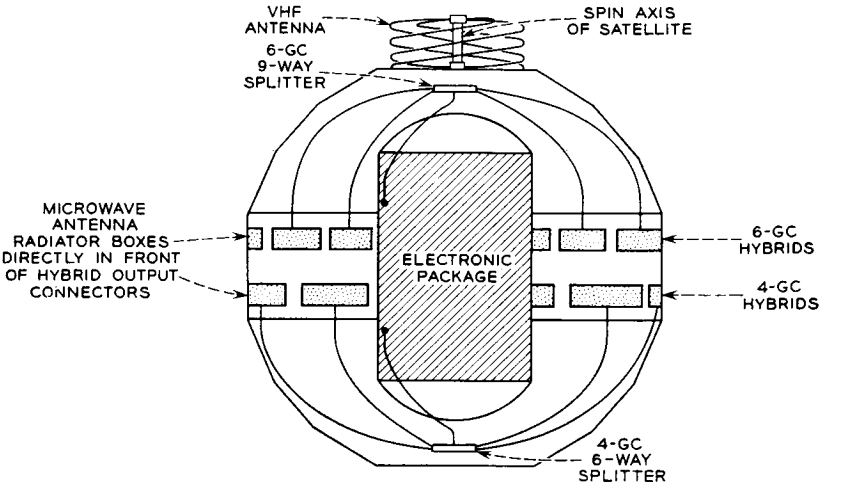

Fig. 2 — Schematic and physical arrangement of antennas in spacecraft.

and semiflexible coaxial cables. The various components of the microwave antenna systems will be described after a brief review of the basic theory underlying this approach.

2.1 *Basic Approach*

D. S. Bugnolo[4] has calculated the surface currents and radiation pattern for a large sphere excited by a great-circle slit. His analysis showed that good axial ratio and nearly isotropic radiation could be maintained to within about 20 degrees of the poles for both the 4-gc and 6-gc frequency bands on a 34.5-inch sphere. A straightforward method for exciting such a slit is by means of a radial disk line fed at the center of the sphere. Unfortunately this feed is impractical for a number of reasons. Bisecting the structures raises severe problems in maintaining structural rigidity between the two halves of the satellite and also impedes the heat flow necessary to minimize thermal gradients within the satellite. Furthermore, the electronic package occupies most of the volume at the center of the spacecraft. Elimination of the continuous radial disk line then suggests the use of some form of discrete approximation such as a belt of individually fed apertures to excite the two halves of the sphere. A further study of the problem revealed that less than one-half db of ripple would be produced in the far field pattern if discrete sources on the great circle were spaced closer than 0.8 wave-

length. For short intervals of time the path between satellite and ground station will intercept a constant latitude on the satellite. In order to avoid amplitude fluctuations of the received signal, the constant latitude of viewing should result in a constant amplitude signal, or the spin axis of the satellite must coincide with the symmetry axis of the radiation patterns. This coincidence can be provided by placing the radiating elements in two closely spaced bands near the equator of the spacecraft, one for the 4-gc transmitter and one for the 6-gc receiver. The use of two bands considerably reduces the individual bandwidth requirements for each set of radiating elements and the associated feed systems.

The variation in field pattern produced by discrete radiating elements near the equator of a sphere is a function of the sphere diameter and the number of elements. After calculating the minimum number of elements needed and allowing some margin, it was decided to employ 72 elements for the 6-gc antenna and 48 for the 4-gc antenna.

Several reservations about the performance of this system using the entire surface of the spacecraft as the radiator remained with the designers until near the end of the development. In particular, no theory was available to predict the interaction between the closely spaced sets of radiating elements at 4 gc and 6 gc and the modification of the radiation pattern by the facets and the solar cells which covered much of the surface area.

2.2 *Radiating Elements*

2.2.1 *Requirements*

Each radiating element must launch a circularly polarized wave over the frequency band of interest and at the same time provide a good impedance match for the feed system.

In view of the great importance of the individual radiating elements to the over-all performance, three alternate designs were considered before concentrating on the most promising one. Only a brief mention will be made of the first two as possibilities for future study.

2.2.2 *Two Early Realizations*

One early design of radiating element consisted of a circular opening on the satellite surface with a circular waveguide recessed into the satellite and fed by a probe from a coaxial line. Between the probe and aperture were two screws forming a quarter-wave plate. This structure worked very well over a wide band so long as sufficient space was pro-

vided between the coaxial probe and the screws forming the quarter-wave plate. Unfortunately, there was not sufficient room in the satellite to allow the circular waveguide to project into the satellite sphere as far as was necessary. When the structure was shortened, the coaxial probe and the quarter-wave plate coupled directly to each other's local fields and strongly interacted with each other. The network could still be tuned to produce circular polarization, but the bandwidth was very small (about 5 mc for a return loss exceeding 20 db).

Another early design proposed the use of a square aperture and waveguide which was excited by two probes, each fed by a coaxial line. By placing an extra 90° phase shift in one of the coaxial lines, circular polarization would be achieved. A serious disadvantage of this structure was the need for twice as many output ports on the power divider and twice as many coaxial connectors as well as provision for the additional 90° phase shift.

2.2.3 *Final Realization*

The final design shown in Fig. 3 employed a rectangular waveguide and aperture with dimensions large enough to propagate two cross-polarized modes (TE_{10} and TE_{01}). Since the two modes have different phase velocities, the length of rectangular waveguide could be adjusted to produce a 90° phase differential between the two polarizations, resulting in circularly polarized fields at the radiating aperture. A single probe was used to feed this structure, and because of space limitations it was decided to introduce the probe from the back wall of the radiating

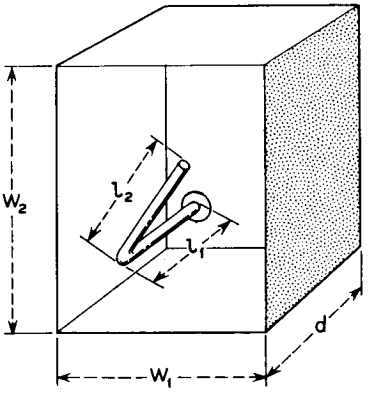

Fig. 3 — Radiating element for microwave antenna.

box. In order to obtain the 90° differential phase shift in as short a length as possible, one cross-sectional dimension of the box was chosen close to cutoff. The lowest frequency utilized in the 4-gc band is 4080 mc. The minimum dimension for propagation of this frequency in empty guide is 1.446 inches, so the narrow dimension was chosen to be 1.500 inches. The other cross-sectional dimension must be somewhat larger to provide a larger propagation constant, but not so large that the radiation patterns for the two polarizations are markedly different. A dimension of 2.100 inches was somewhat arbitrarily selected here. At band center of 4137 mc the two propagation constants are 0.658 radian per inch and 1.613 radians per inch. Therefore, in order to obtain a differential phase shift of $\pi/2$ radians, a path length of 1.65 inches is needed. Since the probe radiates in both directions in the box, some energy goes directly to the apertures and the rest is reflected from the back wall before reaching the aperture. Since there are also reflections from the radiating aperture, the effective path length is rather complex. The depth of the box was experimentally adjusted to 1.490 inches, which gave the best circular polarization for the radiated energy. The optimum axial ratio of the radiated energy is also dependent on the angle of the probe, which is close to 45 degrees.

After obtaining circularly polarized radiation, the remaining problem is to obtain a matched input impedance for the coaxial line. A 50-ohm dielectric bead support for the probe was designed and the two length dimensions of the probe, l_1 and l_2 in Fig. 3, were varied to obtain 50 ohms looking into the coaxial connector at the back of the box. The various adjustments for circularly polarized radiation and good impedance match interact with each other, so that considerable experimentation was found necessary to settle on dimensions which provided the necessary broadband performance. The 4-gc and 6-gc box dimensions are simply scaled in inverse frequency ratio.

Despite early recognition that the radiators would ultimately be magnesium extrusions for high strength-to-weight ratio and precision fabrication, the need for early demonstration of feasibility suggested the use of sheet metal techniques. The first radiating elements were made by cutting 15-mil brass sheet to the right size and shape and bending into the form of a rectangular box having four sides and a bottom, but no top. The adjoining edges were soldered to provide good electrical conductivity. The top edges were bent over at right angles to form lips which could be soldered to the cylindrical supporting midsection in which rectangular holes were punched. The first midsections were made in four parts to permit some tolerance in the associated

hemispheres. A hole was drilled in one corner of the bottom of the box to permit the insertion of a feed probe. The probe was supported by a coaxial connector soldered to the outside of the box bottom. The four quadrant radiator assemblies were fastened between a pair of smooth aluminum hemispheres to form a crude breadboard model. Although the tolerances which had been achieved in the dimensions of the radiators exceeded by several times the estimated allowable tolerances, the first radiation patterns were very encouraging in that they indicated the basic approach was sound, provided the physical structure could be fabricated to the necessary tolerances.

When final models were skillfully fabricated by Dow Metal Products of Bay City, Michigan, the radiating elements were formed as magnesium impact extrusions with a boss on the bottom which was drilled and threaded to serve as the shell of a coaxial connector. Despite the elaborate precautions taken during fabrication to hold the critical dimensions of the radiating elements, small departures from design center values combined in a complicated fashion to cause nonuniform electrical behavior. This problem was solved by shipping test equipment to the factory and selecting satisfactory boxes by measuring return loss over the frequency band of interest. The boxes were then magnesium welded into a wheel-like frame as shown in Fig. 4. During the welding process the frame and boxes were held rigidly in alignment by an elaborate

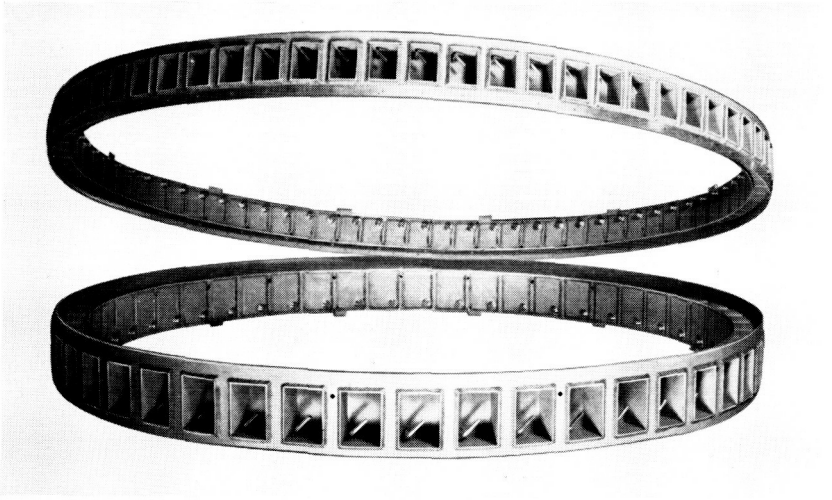

Fig. 4 — Microwave antenna radiating elements assembled into their frames before attachment to the spacecraft.

set of heavy steel jigs. The fixturing is such that when completed, the center of each connector lies within a few thousandths of an inch of a datum plane. The radiating probes were also accurately positioned by means of suitable fixtures before being clamped in place.

2.3 *Feed System of Microwave Antenna*

2.3.1 *Requirements*

Calculations showed that precise microwave distribution systems were required for funneling the 6-gc signals from the 72 receiving radiators to the single receiver within the satellite's electronics package, and similarly for fanning out the amplified 4-gc signals from the satellite's traveling-wave tube to the 48 transmitting apertures. The tolerable variations accumulated within the distributions systems must be restricted to about 15° peak-to-peak and 1 db peak-to-peak, of which no more than 5° and 0.5 db should be systematic.

2.3.2 *Single-Stage Reactive Distribution*

Initially, purely reactive single-stage distribution systems were investigated. These consisted simply of a 48-way power divider for the 4-gc band and a 72-way power divider for the 6-gc band. Each divider was arranged on a circular printed circuit board with a central input connector and the required number of output connectors around the periphery. Early measurements indicated that prohibitive manufacturing tolerances were required, not only for the power dividers themselves, but also for the connecting cables and radiators to keep the phase and amplitude variations within acceptable limits.

2.3.3 *Multistage Reactive and Resistive Distribution*

For the above reason, attention was directed toward multistage distribution systems using suitable resistive type power dividers which would provide isolation between output ports. The so-called resistive dividers are tree-like arrays of lossless hybrids, each with an internal terminating resistance. Furthermore, with this approach more flexibility was possible in the location and weight distribution of the various feed system components within the satellite.

Considering electrical performance alone, the arrangement chosen is one of many alternatives, some of which are undoubtedly better suited for precise microwave power distribution. The choice made resulted from consideration of available space between the radiating elements

and frame structure of the satellite, as well as from such constraints as minimum weight, minimum cross-section (to facilitate free internal heat exchange by radiation between the satellite hemispheres), maximum moment of inertia about the satellite's spin axis (in order to avoid tumbling), etc. The final 4-gc and 6-gc distribution systems chosen are illustrated schematically in Fig. 5. An assembled 72-way power divider for the 6-gc band is shown in Fig. 6. The reactive divider shown at the center is connected by coaxial cables to the nine resistive dividers mounted behind the radiating apertures.

2.3.4 *Reactive Power Dividers*

Centrally located in the 4-gc and 6-gc systems are a 6-way and 9-way reactive power splitter, respectively, connected to 50-ohm input and output cables. These dividers were produced on small circular printed circuit boards, with the input connector centrally located and the 6 or 9 outputs evenly spaced around the periphery as shown by Fig. 7. To maintain 50-ohm impedance levels on both the input and output cables, appropriate $\lambda/4$ transforming sections are incorporated in each of the 6 or 9 output lines near their common junction point. In addition, matching sections are built into the input connector of both the 4-gc

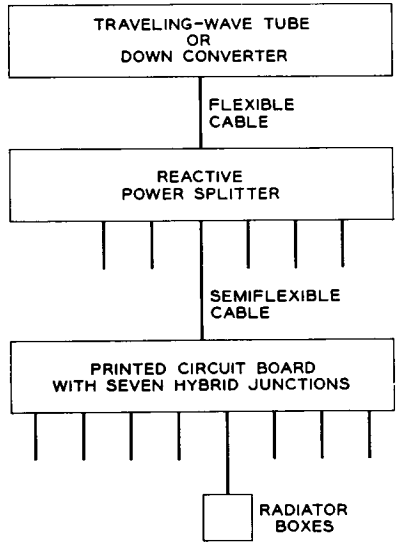

Fig. 5 — Block diagram of microwave antenna feed system.

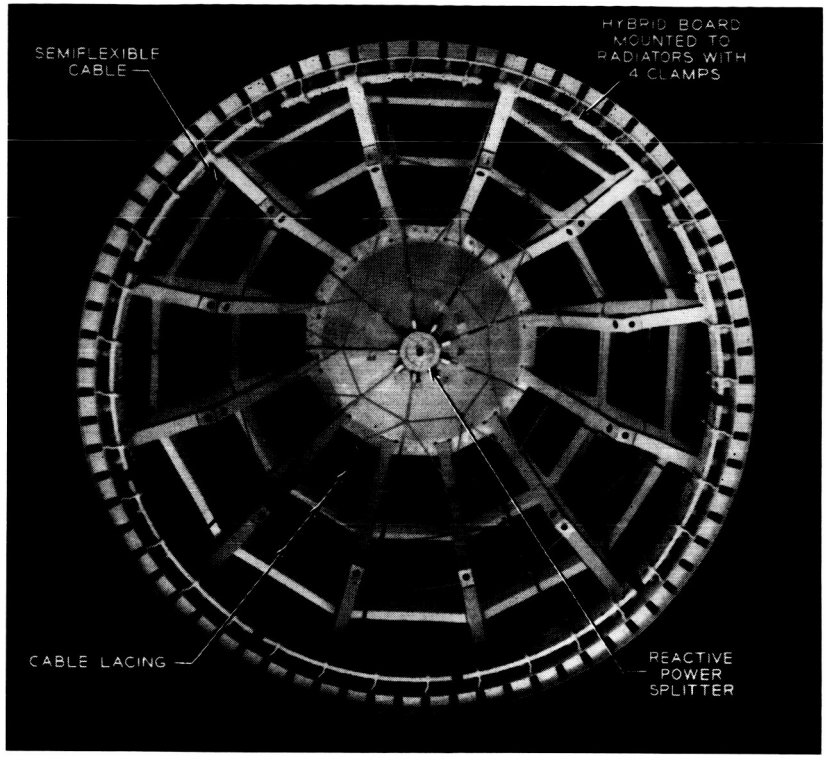

Fig. 6 — View of 6-gc antenna and feed system installed in spacecraft frame.

and 6-gc splitters to provide final over-all tuning of the complete antenna system.

2.3.5 *Resistive Power Dividers (Hybrids)*

Each hybrid board constitutes a resistive 8-way power divider. These hybrid boards are located around the satellite's equator and are curved so as to attach directly to the radiating apertures through special coaxial connectors. In this manner, each hybrid board is rigidly fastened to 8 transmitting or receiving apertures.

The configuration shown in Fig. 8 was chosen for the hybrids, which provides equal power split between ports 2 and 3 independent of frequency. Port 4 is terminated internally by a series resistance of $2Z_0$ (in this case 100 ohms) to maintain isolation between ports 2 and 3.

Fig. 9 shows the center conductor layout for the 4-gc hybrid board,

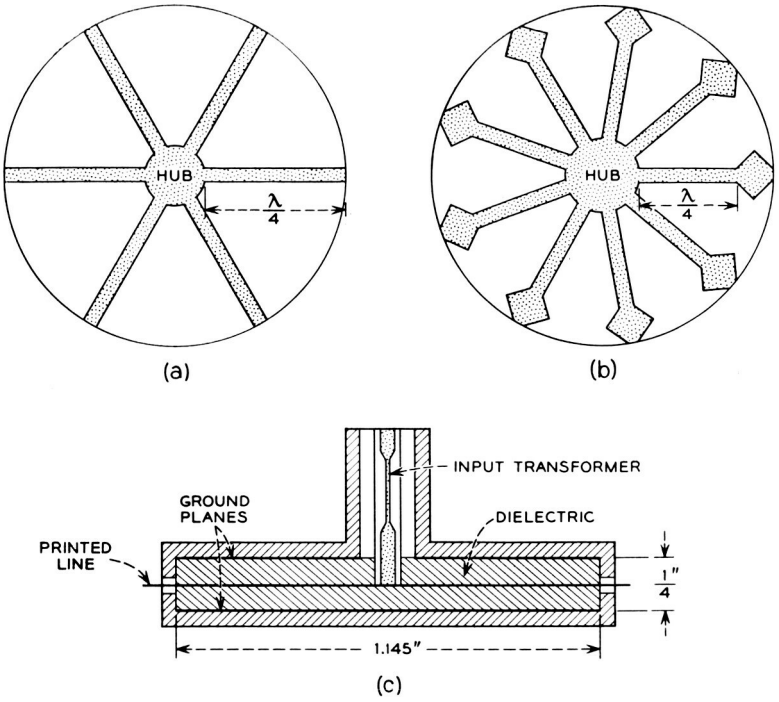

Fig. 7 — Reactive power splitter configuration: (a) 4-gc printed line; (b) 6-gc printed line; (c) cross-section showing input transformer.

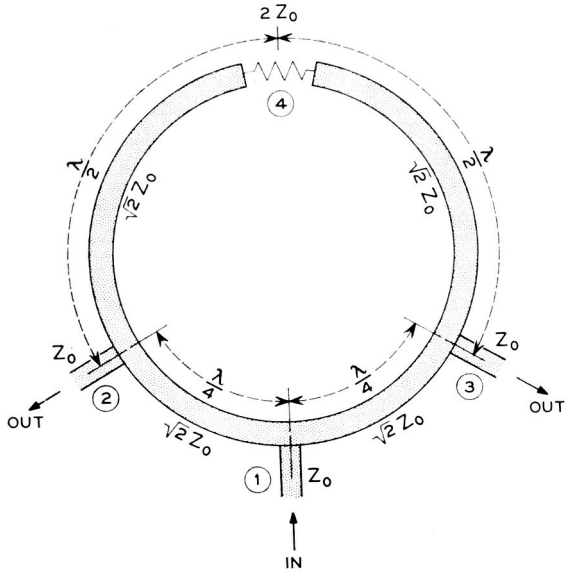

Fig. 8 — Transformed ring hybrid for frequency-independent symmetry.

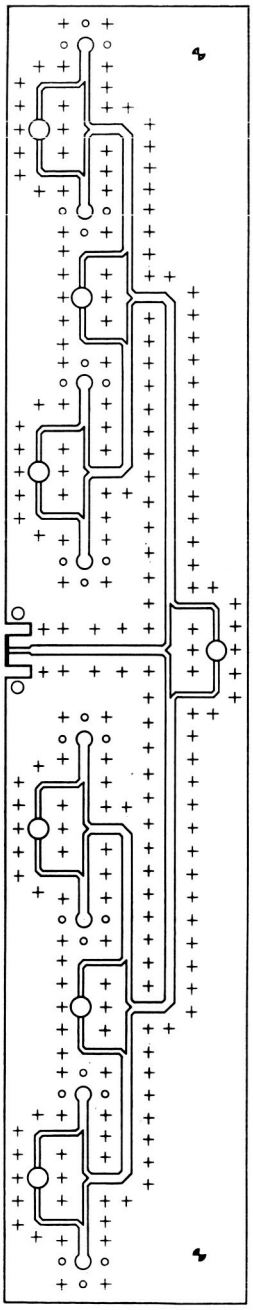

Fig. 9 — 4-ge hybrid printed circuit board.

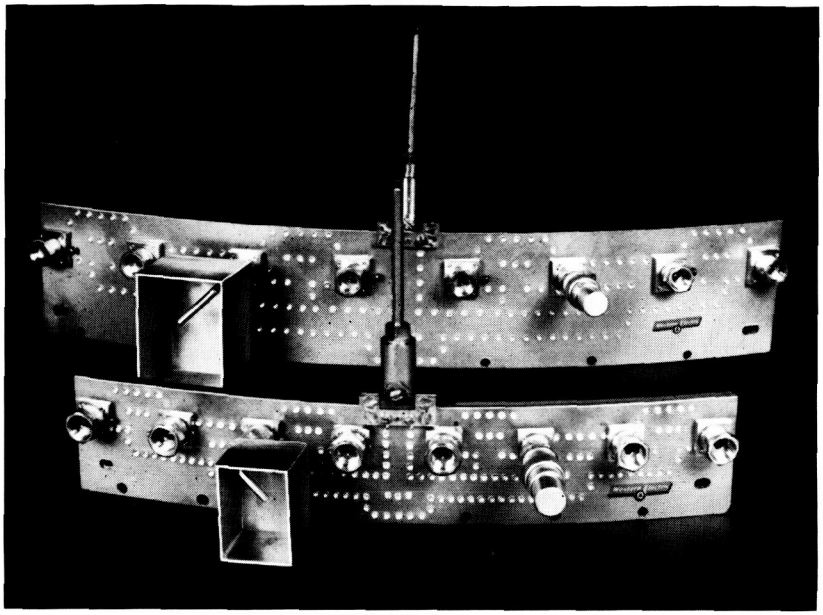

Fig. 10 — 4-gc and 6-gc resistive power dividers.

providing an 8-fold power division by cascading three hybrid stages from input to each output port. The dielectric material used is two sheets of 0.062-inch thick irradiated polyethylene ($\epsilon \approx 2.30$, $\tan \delta \approx 0.00005$). A 100-ohm miniature metal film resistor with flat ribbon leads fits into a circular recess in the dielectric boards and is soft-soldered to the adjoining center conductor to form port 4. Calculations show the absorption loss of the resistors to be $\approx$0.015 db per hybrid at 4 gc and $\approx$0.03 db at 6 gc. Thus, with the three cascaded hybrid stages in each board, the loss due to the 100-ohm resistors is approximately 0.05 db in the 4-gc boards and 0.1 db in the 6-gc boards.

Fig. 10 is a photograph of two assembled hybrid boards — one used at 4 gc and the other at 6 gc. A radiating box is attached to one output port of each hybrid and a short length of 0.160-inch coax is connected to the input ports.

Also noticeable on Fig. 10 are rows of rivets, each 0.090 inch in diameter, which serve both as mechanical fasteners and as electrical shorts around the center conductor, thus ensuring TEM wave propagation without measurable mode conversion. As a rule of thumb, these rivets must be spaced closer than $\lambda/4$ to provide effective shielding and must

be kept away from the center conductor edge by at least one dielectric thickness to prevent changes in characteristic impedance.

These hybrid distribution boards are an interesting use of extremely precise etched circuitry. Stability of performance and distribution of mass were two of the several factors that qualified them for use. The boards are curved riveted "sandwiches" consisting of four layers. The inner two are the dielectric with the etched circuit between them and with copper-clad surfaces adjacent to the outer two magnesium backing plates. All four are riveted together after the boards have been curved to approximately a 16-inch radius. Approximately 200 rivets are used in each board. The large number of rivets, dictated by electrical considerations, results in an extremely rugged and compact circuit board. The boards, 6 for the 4-gc and 9 for the 6-gc antennas, are immediately in back of, and are connected to, the radiating boxes by means of one coaxial connector per antenna box. Fig. 6 shows the hybrid boards as assembled behind the radiating elements. The control of both curvature and the position of the connectors was critical in order to insure proper mating with the radiator box stubs.

2.3.6 *Coaxial Cables*

A total of fifteen semiflexible 50-ohm coaxial cables connect the two central reactive power splitters located near the poles of the satellite to the associated resistive power splitters mounted behind the equatorial arrays of radiating elements. The coaxial is composed of a 43-mil copper wire encased in an irradiated polyethylene dielectric in the form of a helical winding with essentially zero space between turns. The sheath is a copper tube having a diameter of 160 mils and a wall thickness of 5 mils. These cables are sufficiently flexible to be bent so as to follow the contours of the satellite.

2.3.7 *Assembly of Radiating Elements and Feed*

The antenna bands and antenna feed were assembled to the satellite frame in such a manner as to prevent relative motion of the parts at their points of connection. The hybrid boards are rigidly clamped to the antenna bands through the use of four clamps per board, as shown in Fig. 6. The splitters are bolted directly to the frame at its poles and thus are rigidly held. Thus the relative motion that occurs between the hybrids and the splitters during the vibration of launch is accommodated by the bending of the semiflexible cables.

2.4 *Testing and Performance*

2.4.1 *Objectives*

In order to insure the best possible radiation pattern it was necessary to carry out an extensive program of electrical and mechanical tests on the individual components, various subassemblies, and the over-all system. The vital electrical objective is a good pattern, which is insured if microwave power generated or received in the electronics package is transmitted to or from each of the radiating elements with exactly the same phase and amplitude. These tests used a microwave bridge circuit incorporating a calibrated attenuator and phase shifter to measure the relative phase and amplitude between the output ports of the various components of the antennas as well as the over-all antenna assemblies. Phase and amplitude measurement accuracies of the bridge were approximately $\pm 2°$ and ± 0.1 db.

2.4.2 *Radiating Elements*

The radiating elements were checked for axial ratio and return loss over their operating bands. After brief experience with the fabrication of the radiating elements, it was apparent that realistic mechanical tolerances did not insure the necessary uniformity in electrical performance. A sensitive measure of the electrical performance of the individual boxes is the return loss. Return loss measuring equipment (a reflectometer setup) was moved to the fabrication plant, and the boxes were individually tested after they had been welded into the support bands. By electrical tests at the factory it was possible to use boxes in which the mechanical variations combined in a favorable manner and to replace subpar boxes before the whole assembly was removed from the welding fixtures. Although the factory tests indicated the acceptability of the radiators in a qualitative way, it was necessary to make more precise quantitative measurements in the laboratory. Uniformity of transmission through the boxes was checked by exciting them one at a time and terminating the open end of the radiator in a special test fixture. This fixture consisted of a short open-ended rectangular tube of lossy plastic with lips to fit into the mouth of the radiating box and a receiving box mounted on the other end of the tube. With this arrangement, the relative loss and phase of the individual radiators could be compared. These measurements showed a peak-to-peak loss variation of about 0.5 db and a peak-to-peak phase variation of about 8 degrees.

2.4.3 *Reactive Power Dividers*

All the printed circuit reactive power splitters were checked for equality of power division over their operating band. The matching section incorporated at the input to the power splitter was custom designed to allow for individual variations among the reactive and resistive dividers, cables, and radiating elements. The peak-to-peak variation of insertion loss and phase shift taken over the output ports of each splitter is given in Table I.

2.4.4 *Resistive Power Dividers (Hybrids)*

All hybrids boards were given complete electrical testing. Fig. 11 shows the phase and amplitude distribution of all the ports provided by the 4-gc boards; similar results were obtained for the 6-gc boards. Briefly, the peak-to-peak deviations on phase are approximately 8° at 4 gc and 10° at 6 gc, and on amplitude 0.3 db at 4 gc and 0.4 db at 6 gc. In addition, a variation from board to board existed in phase and to a smaller extent in amplitude, which is attributable to lack of precision in the attachment of the input connectors. This phase variation between boards amounted to 10° to 20° and was compensated by corresponding changes in length of the connecting coaxial cable. Input and output VSWR's were measured on all hybrid boards by means of microwave reflectometers and — for more accuracy — on a slotted line. Fig. 12 shows the input and output VSWR's on representative boards. The input match is shown for: (a) radiating elements attached to the output ports and (b) TNC terminations on the output ports. With the TNC terminations, the input VSWR is seen to be less than 1.4 to 1 for about 10 per cent bandwidth. Over the same bandwidths, the output VSWR's are under 1.4 to 1 for the 6-gc boards and under 1.1 to 1 for the 4-gc boards.

2.4.5 *Combined Radiating Elements and Feed*

After individual components, including connecting cables had been measured, the antennas were assembled on the spacecraft framework.

TABLE I—REACTIVE POWER DIVIDERS

Model	Peak-to-Peak Insertion Loss, db	Peak-to-Peak Phase Shift, degrees
Best 4-gc	0.2	1.4
Worst 4-gc	0.4	3.6
Best 6-gc	0.2	4.4
Worst 6-gc	0.55	5.3

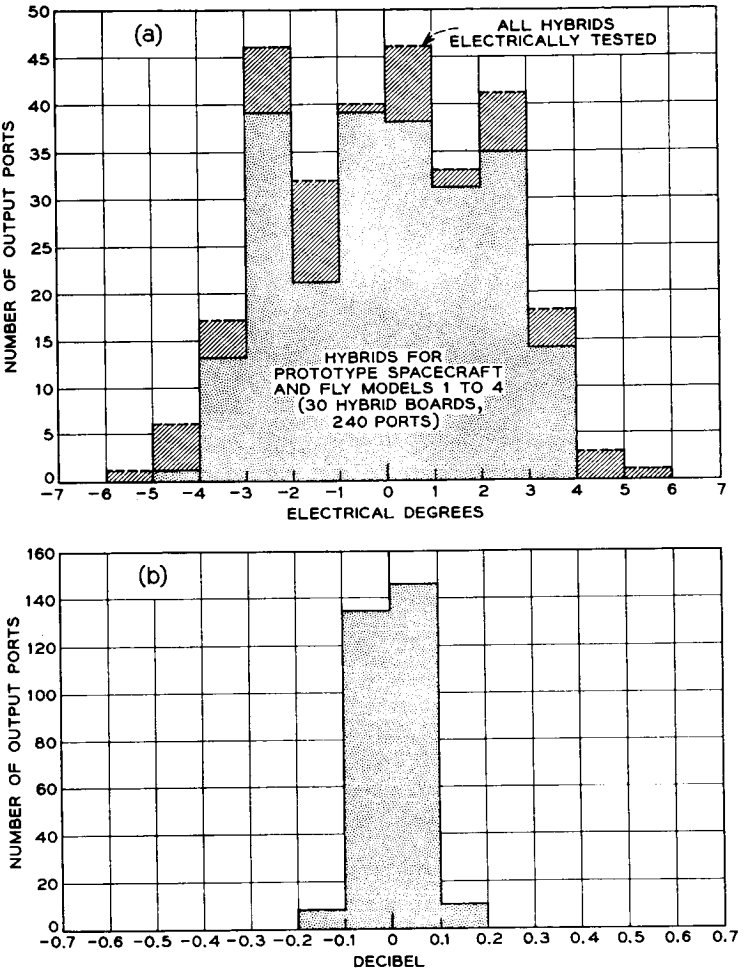

Fig. 11 — Distributions of measurements on the 4-gc hybrid boards: (a) phase distribution; (b) amplitude distribution.

A final check for uniformity of excitation was made of the complete assembly by comparing the phase and amplitude of the individual radiating elements. The test fixture for this purpose consisted of a band of absorbent material to fit around the satellite equator in which was embedded one of the previously described test fixtures for checking the individual radiators. By carefully selecting cable lengths, the average phase to each hybrid group could be accurately matched. This careful selection resulted in peak-to-peak variations as shown in Table II.

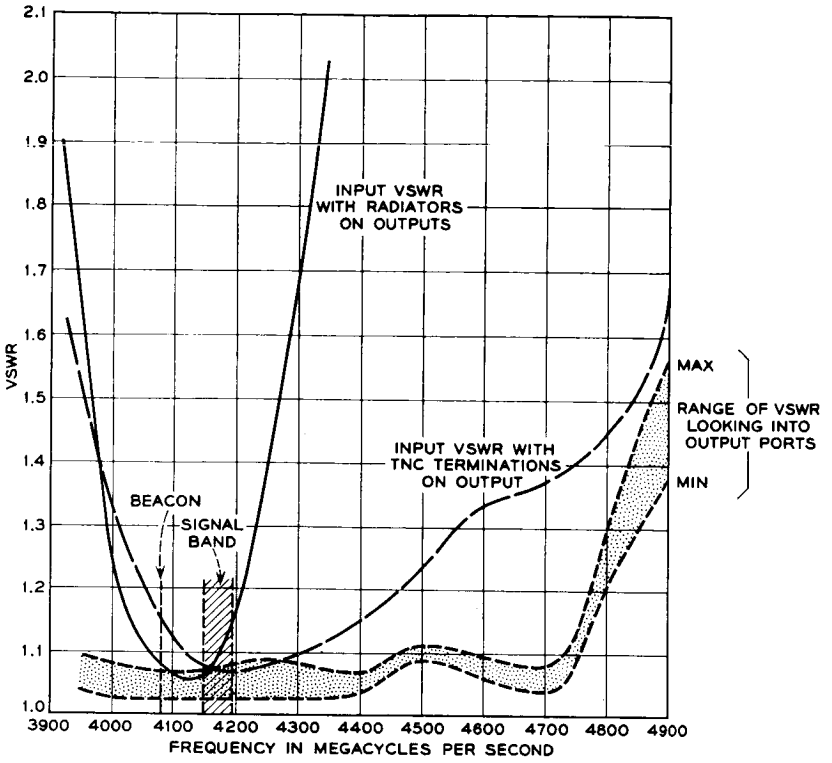

Fig. 12 — VSWR measurements on 4-gc hybrids.

2.4.6 *Over-all Patterns*

Most of the radiation patterns were obtained with an indoor anechoic chamber. These were checked later on an outdoor range with substantial agreement between results. Fig. 13 shows the results for the 6-gc receiving antenna system both for the equatorial and polar aspects. These patterns show the power relative to an isotropic circularly polarized antenna. The all-important equatorial pattern was especially gratifying, because it exhibited a peak-to-peak ripple of less than two db. The

TABLE II — RADIATING ELEMENTS AND FEED

Frequency, mc	Peak-to-Peak Insertion Loss, db	Peak-to-Peak Phase Shift, degrees
4170	1.1 db	10°
6390	1.4 db	14°

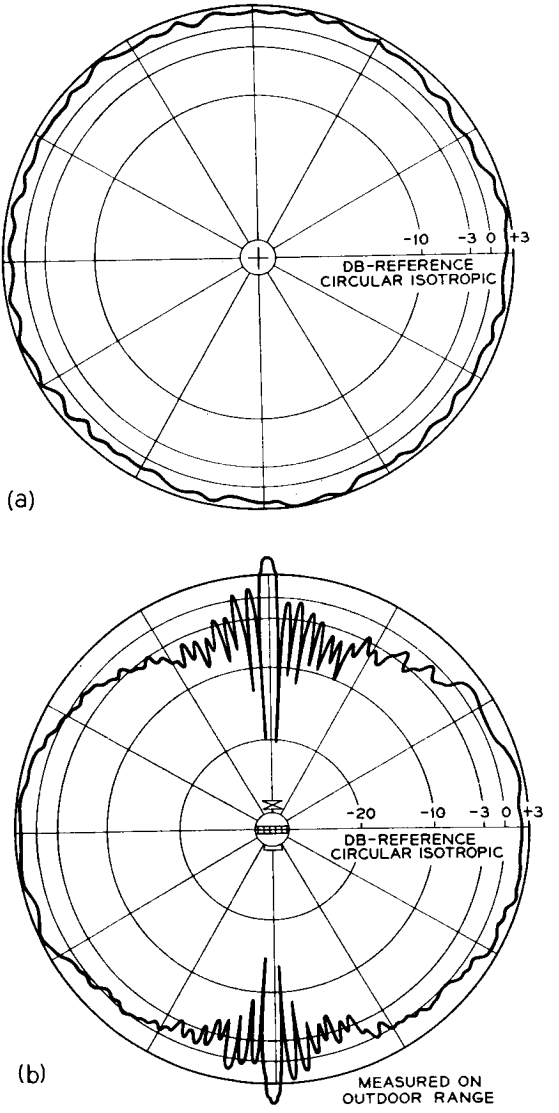

Fig. 13 — Antenna patterns at 6390 mc: (a) equatorial aspect; (b) polar aspect.

polar pattern is reasonably smooth except for the expected nulls near the poles. These patterns show the remarkably large solid angle of coverage provided by these antennas.

Fig. 14 presents the equatorial and polar aspects of the 4-gc transmitting antenna.

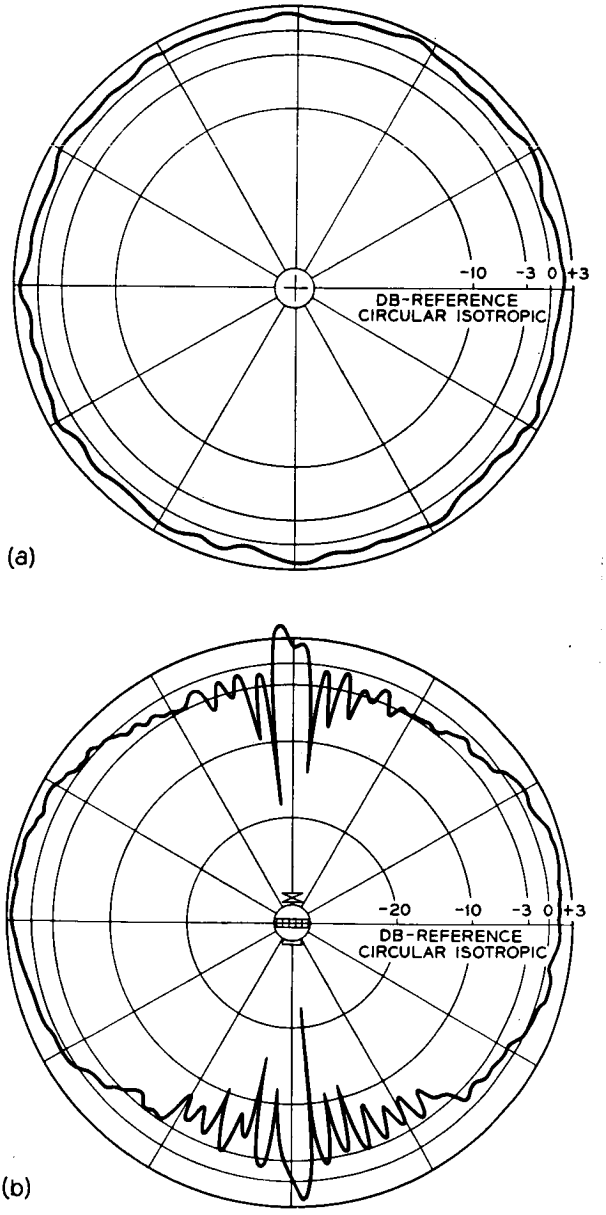

Fig. 14 — Antenna patterns at 4170 mc: (a) equatorial aspect; (b) polar aspect.

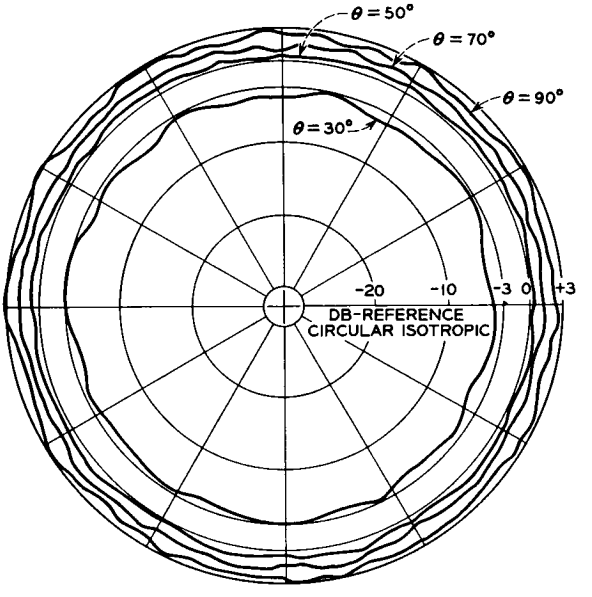

Fig. 15 — Constant-latitude antenna patterns at 4080 mc.

Fig. 15 shows measurements taken at different constant latitudes when measured in an indoor anechoic chamber. The satellite spin produces fluctuations in the received signal level corresponding to the ripples in these patterns. The curve marked $\theta = 90°$ corresponds to the equatorial aspect.

2.4.7 *Thermal and Vibration Considerations*

As pointed out in accompanying papers,[3,5] the spacecraft's spin-axis orientation should be perpendicular to the sun's rays for thermal reasons. The temperature of the antenna components is determined by the actual spin-axis orientation and the duration and frequency of eclipses of the satellite. Extrapolating the predicted skin temperature data in an accompanying article,[5] the temperatures noted in Table III are the ex-

TABLE III — PREDICTED TEMPERATURE EXTREMES

Component	Max. Possible Temp. Range (1 to 2 cycles)	Expected Temperature Range (2000 cycles)
Splitter	+34°C to −50°C	+20°C to −20°C
Hybrid	+10°C to −20°C	+10°C to −5°C
Cables	+40°C to −50°C	+20°C to −10°C

TABLE IV — TEMPERATURE CYCLING CAPABILITIES OF COMPONENTS

Splitter	+40°C to −100°C
Hybrid	+40°C to −100°C
Cables	+65°C to −100°C

tremes predicted, which could only occur once or twice during the satellite's two-year lifetime. In the same table, the temperature extremes are shown for the satellite when the spin axis is within ±30° of being normal to the sun. The range of temperature shown in both extremes includes the effects of full sunlit orbits and maximum eclipse conditions.

Extensive thermal tests were conducted on the hybrids, splitters and antenna cables to ensure that they were capable of withstanding the maximum possible temperature ranges listed above. Table IV is a summary of the temperature cycling capability of the components used in the spacecraft.

Because of the limited development time, extensive tests were not conducted at the more modest "expected temperature range." Based upon an analysis of the stresses which are built up under the extreme temperature cycling conditions and the number of cycles achieved in these tests, it can be confidently predicted that the antenna feed components are capable of withstanding the expected temperature limits for many thousands of cycles.

The thermal tests did disclose a number of weaknesses in the initial designs of the splitters and cables. Mechanical design changes based on these data eliminated the thermal cycling difficulties with the splitters. However, the cable difficulty was more fundamental. In the cable, relative motion occurred between the dielectric and both the inner and outer conductors as a result of temperature cycling. This resulted in a relative displacement of the three items after a few temperature cycles. Different materials and types of cables from a number of suppliers were tested, but all behaved in a similar manner. Through the cooperation of the Tellite Corporation of Orange, N. J., this serious problem was solved by incorporating a helical cut in the dielectric. The depth of the cut extended from the inner conductor to the outer conductor, so that the resulting configuration has a helical winding of dielectric with a small spacing between turns. This design accommodated the difference in expansion between the copper inner and outer conductors and dielectric material.

As a complete assembly the antenna structure was tested thermally in several ways. It was assembled into one of the thermal tester satellites and subjected to temperature cycling as encountered in the environ-

mental test chamber which included solar simulation. The temperature ranges under these conditions were equivalent to the expected temperature range for the high-temperature end, and equivalent to the extremes expected to be encountered for the low-temperature end. In addition, a laboratory test was conducted in which the antenna performance was checked while the poles of the satellite were being cooled down to the extreme low temperature with the antenna radiator section being kept at room temperature. This condition is more severe than that which could be encountered. The antenna satisfactorily passed all these tests.

Section 2.3.7 describes the attachment of the feed to the satellite. In view of the high acceleration levels to which the feed components are subjected and the complex nature of acceleration levels versus the frequency, the most realistic test for mechanical prove-in of the antenna feed structure is on an actual satellite. Hence, the antenna feed system as a whole was vibration tested only after it was assembled into a satellite frame. Accelerometers attached to various portions of the feed system showed a maximum reading at resonance of 260 g on one of the hybrids. Although subsequent electrical tests showed that the antenna systems were still usable, several mechanical weaknesses were uncovered. Further mechanical engineering changes in the mounting of the components eliminated the difficulties.

III. VHF ANTENNA SYSTEM

3.1 *Requirements*

The VHF antenna is used for beacon, telemetry, and command signals. This antenna should be nearly isotropic, have low dissipation loss and radiate circularly polarized waves. The size and position of the antenna is restricted in that it must not shade the solar cells. The VHF antenna is required to operate during the launching of the satellite as well as during orbit. This means that the antenna must radiate with substantially no change in pattern while the satellite is enclosed in the protective fairing and while mounted to the third stage of the rocket during the early phases of the launch. The dimensions of the fiber glass fairing placed upper limits on the height and diameter of the antenna in order to avoid interference during the severe vibration encountered during launch. The final dimensions of the antenna were chosen to make the antenna as large as possible within these restrictions.

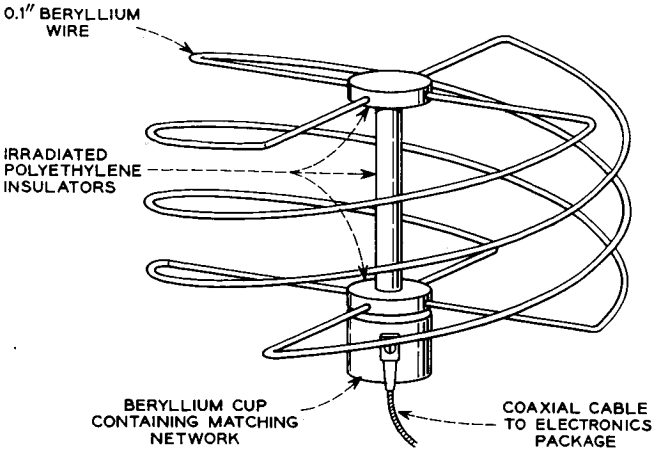

Fig. 16 — Sketch of VHF antenna.

3.2 *Initial Approach*

The decision to mount the communication antennas around the equator of the spacecraft eliminated that position for the VHF antenna. The requirement of nonshading of the solar cells eliminated the use of several sets of crossed dipoles located symmetrically about the satellite. It was therefore originally decided to use a small, multi-element, broadside helix mounted on an erectable mast. A sketch of this helix is given in Fig. 16. The antenna and mast would be collapsed during the launch, since the fairing dimensions would not allow the antenna to be extended, and upon injection into orbit an explosive charge would erect the mast and helix. During the launch a pair of auxiliary dipoles or whips mounted near the south pole of the satellite and fed by means of a directional coupler would maintain telemetry and command capability for the satellite. With this system, which was suggested by Wheeler Laboratories, Smithtown, N. Y., under Bell Laboratories contract, the helix radiated a circularly polarized wave with a pattern similar to that of a short dipole. This gives quite good coverage except near the poles of the satellite.

The helix may be thought of as an end-fed half-wave radiator coiled so as to look like a small loop antenna combined with a short dipole radiator. The loop field is in time quadrature and is at right angles to the dipole field. Circular polarization is obtained by adjusting the dimensions so that the magnitudes of the two field components are equal. The helix was designed by Wheeler Laboratories.[6] The antenna is a

small end-fed radiator with a high input impedance and its bandwidth is relatively small, in fact, considerably smaller than the 13-mc spread between the command and telemetry frequencies. Therefore, a matching network to avoid high standing wave loss was necessary. The dimensions were chosen such that the antenna was resonant at 129 mc, and the matching network provided a conjugate match as well as a transformation of impedance level at both frequencies. A circuit diagram of the matching network is given by Fig. 17.

Beryllium wire 0.1 inch in diameter was chosen to wind the helix because of its light weight and rigidity. A thin layer of gold was plated over the beryllium to reduce its dissipative loss. In order to provide the proper coefficient of emissivity to aid in the thermal balance of the spacecraft, the exterior portion of the antenna system was sprayed with an aluminum oxide coating by a plasma gun.

During the development a number of uncertainties arose to make an antenna on an erectable mast seem less and less desirable. The adverse effect on the moment of inertia was compounded, since the stringent requirements on the helix dimensions dictated elaborate jigs to insure these dimensions after the stress of launch and upon erection. The collapsed helix, while not a good radiator, did radiate enough to affect the patterns of the dipoles to an unpredictable extent if the vibration during launch caused the helix elements to intermittently touch one another. Also, the dipoles themselves affected the in-orbit pattern, not so much near the equator, but noticeably in the vicinity of both poles.

3.3 *Final Approach*

Because of these uncertainties it was decided to use the helix as a short vertically polarized dipole permanently mounted to the north pole of the satellite. Since the ground antenna used for the command and telemetry signals is circularly polarized, the problem of polarization

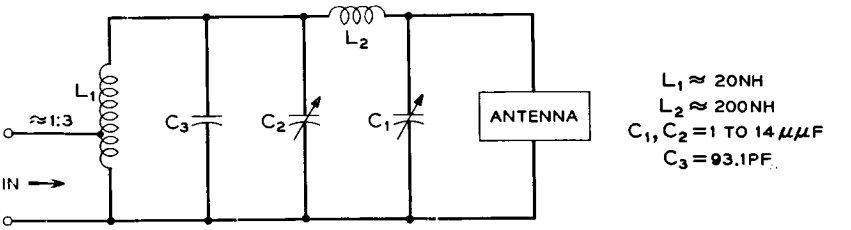

Fig. 17 — Schematic diagram of VHF antenna matching network.

tracking does not arise if the system can tolerate the additional 3-db loss. A careful study of the signal levels and path losses showed essentially no penalty for commandability and a small penalty for telemetry. Mounting the helix directly on top of the satellite resulted in the following advantages:

(a) Since the helix is not collapsed during launch, the whips and associated directional coupler can be eliminated.

(b) Since the helix is directly on the sphere, the additional cable length required for the erectable mast is eliminated. This results in a 0.5 db decrease in loss.

(c) The elimination of the mast erecting package results in an increase in reliability since the antenna would have been useless had the firing mechanism failed.

Since mounting the helix directly on top of the satellite destroys the balance between the loop and dipole radiation components, the dimensions were altered to insure that it would fit into the launch fairing, yet retain the same impedances. This alteration did not change the matching network and left the dipole component unaffected.

The matching network was adjusted while mounted on a model of the satellite. The model was mounted on the roof of the Hillside, N. J., laboratory, and final adjustments were made with the base of the helix and the network cup surrounded by dry ice; a thermocouple attached to the network cup indicated −75°C. Fig. 18 shows that the match at both frequencies is degraded as the temperature increases, but the

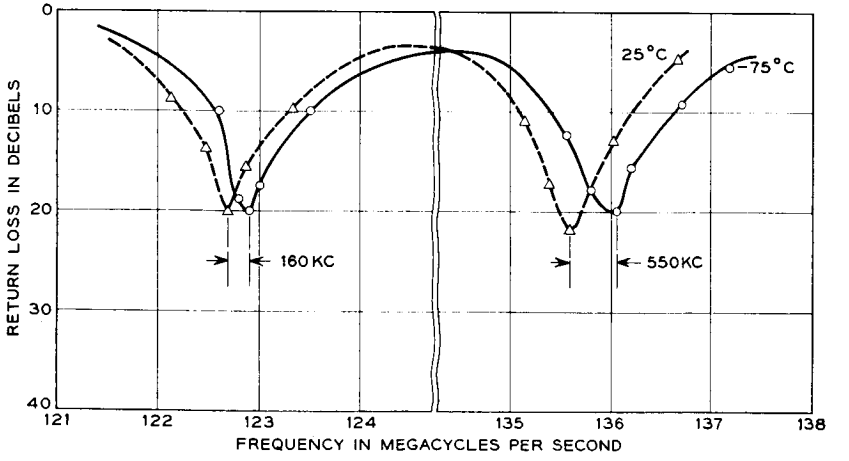

Fig. 18 — Return loss measurements of VHF antenna.

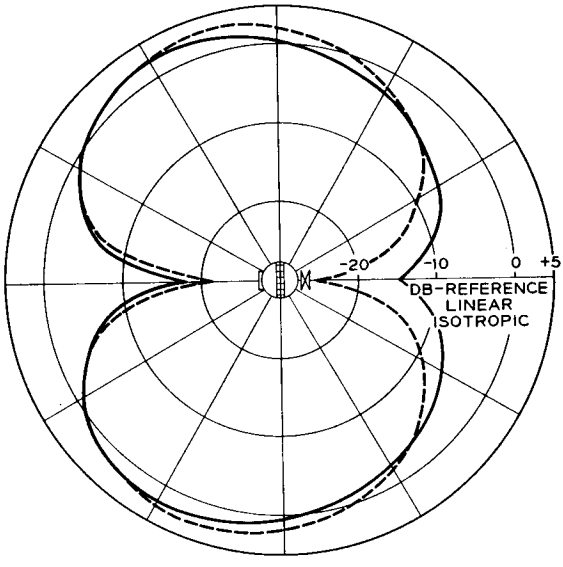

Fig. 19 — Polar aspect VHF antenna pattern at 123 mc: solid curve—measured pattern; dotted curve—calculated pattern.

antenna is still quite usable at +25°C, although, except at launch, it is never expected to be warmer than −50°C.

3.4 *Testing and Performance*

The radiation patterns of the antenna are perfectly uniform when viewed at a constant latitude and when the satellite is rotated about its spin axis. The pattern does vary as the satellite is rotated at right angles to the spin axis, as is shown by Fig. 19. This figure shows the radiation pattern at approximately 123 mc as well as a theoretical pattern assuming a lossless antenna. The differences in maximum gain points indicate a loss in the matching network and dissipation loss in the helix of 1.5 db at approximately 123 mc. The corresponding comparison at approximately 136 mc shows a loss of 2.5 db.

IV. CONCLUSION

Two high-performance, isotropic, circularly polarized, microwave antenna systems have been designed, constructed, and operated successfully in the environment of outer space. The radiation patterns demonstrate that by use of extremely precise techniques of magnesium

fabrication and printed wiring a spherical surface can be uniformly excited by as many as seventy-two discrete radiating elements.

In addition, reliable and efficient narrow-band radiation of VHF signals has been achieved by employing a multi-element helix with a matching network.

V. ACKNOWLEDGMENT

The authors wish to pay tribute to their many colleagues in Bell Telephone Laboratories and Western Electric who devoted their skill and energies far beyond the call of duty in making this development possible. Special mention should also be made of the wholehearted cooperation of many companies outside the Bell System.

REFERENCES

1. Dickieson, A. C., The *Telstar* Experiment, B.S.T.J., this issue, p. 739.
2. Hoth, D. F., O'Neill, E. F., and Welber, I., The *Telstar* Satellite System, B.S.T.J., this issue, p. 765.
3. Shennum, R. H., and Haury, P. T., A General Description of the *Telstar* Spacecraft, B.S.T.J., this issue, p. 801.
4. Bugnolo, D. S., A Quasi-Isotropic Antenna in the Microwave Spectrum, I.R.E. Trans. on Ant. and Prop., **AP-10,** No. 4, July, 1962.
5. Hrycak, P., Koontz, D. E., Maggs, C., Unger, B. A., Stafford, J. W., and Wittenberg, A. M., The Spacecraft Structure and Thermal Design Considerations, B.S.T.J., this issue, p. 973.
6. Wheeler, H. A., A Helical Antenna for Circular Polarization, Proc. I.R.E., **35,** December, 1947, p. 1484.